Calibration of Thin Heat Flux Sensors for Building Applications Using ASTM C 1130

By

Robert R. Zarr and Brian P. Dougherty
Building and Fire Research Laboratory

Dr. James J. Filliben
Statistical Engineering Division
National Institute of Standards and Technology
Gaithersburg, MD 20899-8632 USA

And

Víctor Martínez Fuentes
División de Termometría
Centro Nacional De Metrologia
km 4,5 carretera a los Cues
El Marqués, Qro. 76241
Mexico

Reprinted from the Journal of Testing and Evaluation, May 2001.

NIST
National Institute of Standards and Technology

Robert R. Zarr,[1] *Victor Martinez-Fuentes,*[2] *James J. Filliben,*[3] *and Brian P. Dougherty*[1]

Calibration of Thin Heat Flux Sensors for Building Applications Using ASTM C 1130

Authorized Reprint from Journal of Testing and Evaluation, May 2001 ©Copyright 2001
American Society for Testing and Materials, 100 Barr Harbor Drive, West Conshohocken, PA 19428-2959

REFERENCE: Zarr, R. R., Martinez-Fuentes, V., Filliben, J. J., and Dougherty, B. P., **"Calibration of Thin Heat Flux Sensors for Building Applications Using ASTM C 1130,"** *Journal of Testing and Evaluation,* JTEVA, Vol. 29, No. 3, May 2001, pp. 293–300.

ABSTRACT: Calibration measurements of thin heat flux sensors for building applications are presented. The findings support the continued development of precision and bias statements for ASTM Practice C 1130. Measurements have been conducted using a 1016 mm diameter guarded hot plate apparatus (Test Method C 177) from 10°C to 50°C and for a heat flux range of ±13 W/m^2. The option of using a 610 mm heat flow meter apparatus (Test Method C 518) to calibrate the heat flux sensors is also explored. Experimental designs are presented to compare test methods, evaluate which parameters affect the sensor output, and determine the functional relationship between the sensor output and applied heat flux. The study investigates two sizes of sensors fabricated by one manufacturer. Sensor equivalency, grouped by size, is evaluated to determine whether a calibration based on a subset of sensors will suffice or if extensive individual calibrations are needed.

KEYWORDS: building technology, calibration, guarded hot plate, heat flow meter, heat flux sensor, repeatability, thermal conductance, thermal insulation

The National Institute of Standards and Technology (NIST) recently completed a series of calibration tests of twelve thin heat flux sensors. The sensors are being used to investigate the thermal performance of building-integrated solar photovoltaic panels [*1*]. The calibration data provide valuable information for the development of precision and bias statements for ASTM Practice for Calibrating Thin Heat Flux Transducers (C 1130). Practice C 1130 describes experimental procedures for the calibration of heat flux sensors for use on industrial equipment or building envelope components. For an application on an insulated building component, calibration at low levels of heat flux, on the order of 20 W/m^2 or less, is appropriate.

This paper describes the heat flux sensors, test methods, and an analysis of four calibration issues of interest to the user of C 1130: (1) sensor equivalency, (2) linearity and temperature effects, (3) uncertainty analysis, and (4) test method suitability. The issue of sensor equivalency seeks to answer the question: can a calibration developed from a subset of sensors be used or are individual calibrations required for each sensor? Another major objective of the analysis is the investigation of the sensitivity and linearity of the sensors, and the effect of other factors, particularly temperature. An assessment of uncertainties for the calibration results is also provided. The final section of the paper explores the option of using two ASTM test methods for calibrating the same sensors.

Manuscript received 6/16/2000; accepted for publication 11/29/2000.

[1] Mechanical engineer, National Institute of Standards and Technology, 100 Bureau Drive, Gaithersburg, MD 20899-8632.

[2] Mechanical engineer guest worker, National Center of Metrology, Km 4.5 Carretera a los Cues, El Marques, Queretaro 76900, Mexico.

[3] Mathematical statistician, National Institute of Standards and Technology, 100 Bureau Drive, Gaithersburg, MD 20899-8980.

Background

This section describes the heat flux sensors, ASTM test methods, and test protocols for calibration.

Sensors

Table 1 summarizes the physical characteristics of the heat flux sensors. Each sensor utilizes a thermopile that produces an electrical voltage as a function of the heat flux through the metre area of the sensor. The underlying principle of operation is based on the Seebeck effect [*2*]. The sensors were manufactured using printed circuit techniques so that the metal junctions of the thermoelements were placed in the same geometric plane. In operation, the different thermal conductivities of the constitutive elements perturb the local heat flux through the sensor's metre area producing a tangential temperature gradient [*3*] and electrical output voltage for the sensor.

ASTM Test Methods

Practice C 1130 provides experimental procedures for the calibration of heat flux sensors. For this study, two test methods were utilized—Test Method for Steady-State Heat Flux Measurements and Thermal Transmission Properties by Means of the Guarded-Hot-Plate Apparatus (C 177) and Test Method for Steady-State Heat Flux Measurements and Thermal Transmission Properties by Means of the Heat Flow Meter Apparatus (C 518). Test method C 177 is considered a primary (or absolute) method, whereas C 518 is a comparative method since specimens of known thermal transmission properties are required for calibration of the apparatus. The calibration procedures for the C 518 apparatus are discussed in the literature [*4,5*]. Table 2 summarizes the important characteristics of each apparatus.

Test Protocol

The heat flux sensitivity, H (μV per W/m^2), is the ratio of the sensor's output voltage, E (V), and the one-dimensional heat flux, q (W/m^2), through its metre area, or

$$H = \frac{E}{q} \times 10^6 \tag{1}$$

When calibrating a sensor, q is provided by the test apparatus and, under steady-state conditions, is a function of the thermal conduc-

TABLE 1—*Heat flux sensors.*

Characteristics	Small (A)	Large (B)
Quantity	9	3
Dimensions, mm	500 by 500	610 by 610
Metre area, mm	250 by 250	305 by 305
Nominal thickness, mm	0.8	0.8
Number of junctions	2500	3600
Nominal resistance, Ω	1500	2250
Metal junctions	Copper-Constantan	Copper-Constantan
Substrate material	Glass-fiber reinforced epoxy	Glass-fiber reinforced epoxy

TABLE 2—*Apparatus characteristics.*

Characteristics	C 177 (Guarded Hot Plate)	C 518 (Heat Flow Meter)
Plate size, mm	1016 (diameter)	610 by 610
Metre area, mm	406 (diameter)	250 by 250
Time to achieve steady-state, h	8	4

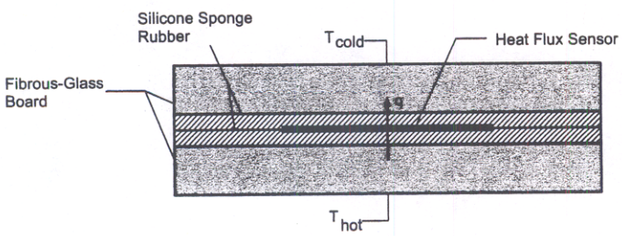

FIG. 1—*Heat flux sensor test assembly.*

tance (C) of the specimen and the applied temperature difference (ΔT),

$$q = C\Delta T \tag{2}$$

The calibration temperature (T) is the average of the apparatus hot and cold surfaces. For C 177, q was obtained from the ratio of the specimen heat flow (Q) and the metre area (A). The specimen heat flow (Q) was determined from the product of the metre area input voltage (V) and corresponding current (i). For C 518, q was determined from the product of the apparatus calibration factor [*4,5*] and the output voltage of the apparatus heat flux transducer.

Each sensor was calibrated individually between adjacent layers of 3 mm silicone rubber (470 kg/m^3) and 25 mm fibrous-glass thermal insulation (135 kg/m^3) as shown in Fig. 1. This technique embedded the sensor in an assembly that provided a thermal conductance similar to the end-use application. The assembly was inserted between the hot and cold plates of the apparatus, compressed a minimum of 2%, and tested with a steady temperature difference applied at the outer surfaces of the assembly. At the conclusion of a test, the assembly was dissembled and the sensor removed. The same assembly materials were reassembled with a different sensor and the process repeated.

Usually, the sensor's metre area is calibrated within the perimeter of the metre area of the apparatus. As noted in Tables 1 and 2, the metre areas of the small sensors are within or equal to the metre areas of the apparatus. For the large sensors, less than 1% of the sensor metre area is outside the metre area of C 177. Given that more than 99% of the sensor's metre area is within the metre area of C 177, the latter procedural deviation was considered small and subsequently neglected. Unfortunately, approximately 33% of the metre area of the large sensors is outside of metre area of C 518 and this deviation is discussed in the analysis.

A thin thermocouple (copper-constantan) was installed at the center of each heat flux sensor to monitor the sensor temperature (T_1). The output voltages (E) and temperatures (T_1) of the sensors, as well as q, T, and ΔT from the respective apparatus, were collected at 1 min intervals for 1 h using separate commercial data acquisition systems. The standard uncertainties for the above measurements are discussed in the Appendix.

As a side note, for building applications, the parameter of interest when utilizing heat flux sensors is the multiplicative inverse of the heat flux sensitivity, that is ($1/H$). The uncertainty contributions associated with end-use application are not addressed in this paper. However, for reference, other researchers have estimated the uncertainty for field applications to be as much as ±10% [*6*].

Analysis

The analysis of data addressed four questions. First, can the sensors be treated equivalently in order to develop a global calibration (i.e., based on a subset of sensors), or are individual calibrations required? Second, what is the functional form of the calibration equation? Third, what is the standard uncertainty for the estimates of H? Fourth, do Test Methods C 518 and C 177 yield equivalent results for calibration?

Sensor Equivalence: Global versus Individual Calibration

The primary objective of the individual calibrations at fixed thermal conditions was to assess and quantify the equivalency of the heat flux sensors. If the sensors were, in fact, deemed equivalent, a global calibration could then be investigated. If not, a more extensive calibration would be required. A secondary objective was to determine the repeatability of Test Method C 177 as part of Practice C 1130. To determine repeatability, the same operators conducted replicate measurements for several sensors on different days. Completion of all measurements required nearly 30 days.

To assess the sensor-to-sensor variation, individual measurements were conducted using C 177 at 20°C and a heat flux of 5.9 W/m^2 through the assembly. For the test setup, the thickness of the assembly was preset to 58.9 mm, compressing the assembly by 2%. During the test, secondary factors such as the clamping force and chamber ambient humidity were monitored, but not fixed. The mean clamping force for all tests was 414 N ± 40 N (one standard deviation) and the relative humidity was less than 10%.

Table 3 gives the test data and summary statistics arranged by sensor size (A, B) for T, ΔT, q, T_1, E, and H. For consistency, a negative sign (−) has been assigned to values of q and ΔT when values of E were negative. The summary statistics indicate that test-to-test variations for the plate temperatures and corresponding heat fluxes (T, ΔT, and q) were quite small and that the coefficients of variation (%CV) for H were also small, less than 1.3% for A and 0.5% for B. The mean heat flux sensitivities ($\bar{H}$) were 93.6 μV/(W/m^2) and 135.6 μV/(W/m^2) for A and B sizes, respectively. The value of $\bar{H}$ for the small sensors is within 2% of results previously reported by another researcher for a similar sensor [*3*].

Figure 2 plots the relative difference between values of E (Table 3) and the group means ($\bar{E}$) by sensor size (A, B). No apparent trends are observed in the data. The maximum variation among the

TABLE 3—*Sensor-to-sensor variation using Test Method C 177.*

Date	Heat Flux Sensor	T, °C	ΔT, K	q, W/m^2	T_1, °C	E, V	H, μV/(W/m^2) Sensor
11/03/99	A1	20.00	−10.00	−5.892	19.95	−0.000552	93.8
10/27/99	A2	20.00	−10.00	−5.873	19.96	−0.000562	95.7
11/15/99	A2	20.00	−10.00	−5.877	19.98	−0.000555	94.5
11/09/99	A3	20.00	−10.00	−5.911	19.94	−0.000552	93.4
11/16/99	A3	20.00	−10.00	−5.878	19.95	−0.000555	94.4
11/18/99	A3	20.00	−10.00	−5.879	19.95	−0.000555	94.4
11/22/99	A3	20.00	−10.00	−5.882	19.95	−0.000555	94.3
10/30/99	A4	20.00	−10.00	−5.891	19.95	−0.000542	92.1
11/17/99	A4	20.00	−10.00	−5.882	19.95	−0.000544	92.4
11/02/99	A5	20.00	−10.00	−5.905	19.97	−0.000540	91.5
11/01/99	A6	20.00	−10.00	−5.900	19.95	−0.000538	91.3
11/24/99	A6	20.00	−10.00	−5.874	19.95	−0.000540	91.9
10/31/99	A7	20.00	−10.00	−5.902	20.01	−0.000563	95.4
10/28/99	A8	20.00	−10.00	−5.872	19.99	−0.000546	93.0
10/29/99	A9	20.00	−9.99	−5.878	19.95	−0.000556	94.5
11/19/99	A9	20.00	−10.01	−5.888	19.95	−0.000553	93.9
11/05/99	B10	20.00	−10.00	−5.883	19.95	−0.000798	135.7
11/08/99	B11	20.00	−10.00	−5.900	19.94	−0.000796	134.9
11/23/99	B11	20.00	−10.00	−5.884	19.94	−0.000797	135.5
11/04/99	B12	20.00	−10.01	−5.907	19.94	−0.000806	136.4
Summary Statistics (A,B)							
Mean	A	20.00	−10.00	−5.886	19.96	−0.000551	93.6
Std.	A	0.002	0.004	0.012	0.018	0.000007	1.2
% CV	A	0.0	−0.1	−0.2	0.1	−1.2	1.3
Mean	B	20.00	−10.00	−5.894	19.94	−0.000799	135.6
Std.	B	0.002	0.003	0.012	0.002	0.000005	0.6
% CV	B	0.0	−0.0	−0.2	0.0	−0.6	0.5

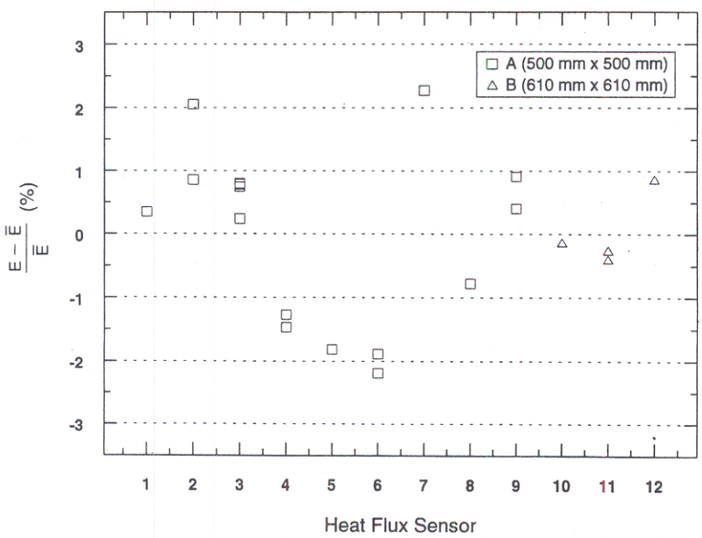

FIG. 2—*Sensor-to-sensor variation using Test Method C 177:* ($\Delta T = -10$ *K*, $T = 20°C$, $q = -5.9$ *W/m*^{2}).

small sensors (A) was less than ±2.5% and for the large sensors (B) less than ±1%. Given that the relative differences in Fig. 2 and coefficients of variation for H (Table 3) are small in comparison to the uncertainties of the end-use application (±10%) [*6*], we conclude that the sensors are equivalent and thus a global calibration among sensor sizes is appropriate.

By pooling replicate data and weighting with their respective degrees of freedom, the repeatability standard deviations were determined to be 0.53 μV/(W/m^2) (0.6%) and 0.40 μV/(W/m^2) (0.3%) for A and B sensors, respectively. The larger value is used later to determine the combined standard uncertainty for H.

Calibration Curve

The purpose of this section is to develop a calibration curve that relates E and q, i.e., $E = f(q)$. In this regard, the following questions are addressed: (1) Are other variables needed, in particular T_1 to fully relate E and q, i.e., $E = f(q,T)$? (2) Is an interaction term

qT needed? (3) If q itself is sufficient, is the relationship between E and q linear? and, (4) If linear in q, is an intercept term needed?

Temperature Effect on the Calibration—Other researchers [7] have identified various parameters that can affect the sensor output (E). These parameters include heat flux (q), temperature (T), clamping force, thermal conductivity of surrounding material(s), surface air velocity, emittance of the sensor and surrounding material(s), moisture, and installation. Other parameters not specifically mentioned could also affect sensor output but are not considered in this study. The objective of this part of the study was to determine the effect of two such factors, q and T. Note that q was varied by indirectly controlling a surrogate parameter, that is, the ΔT across the assembly. A complication was that the thermal conductance (C) of the assembly is a function of temperature (i.e., $C = C(T)$), and therefore changes in T also affected q and therefore E (see Eqs 1 and 2).

The findings from the previous section permitted the selection of a subset of sensors for full characterization as a function of q and T. Therefore, two small sensors were selected *randomly* and tested individually in the same assembly (Fig. 1) using C 177 at four levels each of q (ΔT) and T. The ranges for q (± 13 W/m^2) and T (10 to 50°C) were selected to represent end-use conditions. For the test setup, the thickness of the assembly was again preset to 58.9 mm, compressing the assembly 2%. The clamping force and thickness varied with temperature due to thermal expansion effects from test to test.

Table 4 summarizes the test results for the 16 tests. For consistency, a negative sign (−) has again been assigned to values of q (and ΔT) for negative values of E, indicating a change in the direction of heat flow. The choice for electrical polarity was entirely arbitrary; inverting the sensor changes the direction of heat flow and produces a positive signal.

The data in Table 4 were fit to the following model

$$E = a_0 + a_1 q + a_2 T_1 + a_3 q T_1 + \varepsilon \quad (3)$$

where q is the heat flux (W/m^2), T_1 is the sensor temperature (°C), a_i are the regression coefficients, and ε is a random error term. To test the statistical significance of the estimates for the individual regression coefficients, 95% confidence intervals (CI) were constructed for a_i. The form of the confidence interval is

$$\hat{a}_i \pm t_{0.975,n-p}\, Std(\hat{a}_i) \quad (4)$$

TABLE 4—*Effect of temperature and heat flux on small sensors (A).*

Index	Heat Flux Sensor	T,°C	ΔT, K	q, W/m^2	T_1, °C	E, V
1	A7	10.00	−20.00	−11.443	10.20	−0.001079
2	A7	50.00	−20.00	−13.266	49.76	−0.001245
3	A7	10.00	19.99	11.464	10.29	0.001080
4	A2	50.00	−20.00	−13.253	49.71	−0.001240
5	A2	10.00	20.00	11.465	10.21	0.001073
6	A2	50.00	20.00	13.141	49.89	0.001240
7	A2	10.00	−20.00	−11.465	10.18	−0.001080
8	A7	50.00	20.00	13.161	49.87	0.001244
9	A7	20.00	−10.00	−5.881	20.01	−0.000560
10	A2	39.99	−10.01	−6.344	39.79	−0.000595
11	A2	20.00	10.00	5.874	20.00	0.000554
12	A7	40.00	9.99	6.309	39.90	0.000597
13	A2	20.00	−10.00	−5.871	19.97	−0.000558
14	A7	40.00	−10.00	−6.332	39.82	−0.000601
15	A7	20.00	10.00	5.865	20.05	0.000561
16	A2	40.00	10.00	6.330	39.83	0.000594

TABLE 5—*Hypothesis test for statistical significance of regression coefficients.*

	a_0	a_1	a_2	a_3
$\hat{a}_i$	−3.91E-06	9.43E-05	1.44E-07	−3.03E-09
$Std(\hat{a}_i)$	2.55E-06	2.48E-07	7.54E-08	6.68E-09
$t_{0.975}$, n-p	2.145	2.145	2.145	2.145
95% CI−	−9.38E-06	9.38E-05	−1.71E-08	−1.74E-08
95% CI+	+1.56E-06	9.48E-05	+3.06E-07	+1.13E-08
Conclusion	Insignificant	Significant	Insignificant	Insignificant

where n (= 16) is the number of data points, p (= 4) is the number of parameters in Eq 3, $t_{0.975,n-p}$ is the 97.5 percentile of the Student's t-distribution with $n - p$ degrees of freedom, and Std($\hat{a}_i$) is the standard deviation of the estimated regression coefficient $\hat{a}_i$. If the interval defined by Eq 4 contains zero, then the coefficient of interest is statistically insignificant at the $\alpha = 0.05$, where 95% = 100(1 − α). From Table 5, at $\alpha = 0.05$, we conclude that only the q coefficient (a_1) is statistically significant.

Unfortunately, the confidence interval technique alone cannot detect the presence of a temperature effect if subtle. For this case, further analysis is required. Using the results from Table 5, we tentatively assume the simple model, $E = a_1 q$, and fit this model with the data from Table 4. If this model is entirely adequate, the deviations (defined as the differences of the data and predicted values) should be random, without structure, when plotted against the other variables, such as T or qT. Conversely, if the model is inadequate, the deviations will exhibit a deterministic structure when plotted against such contributing variables.

Figure 3 plots the deviations (from the $E = a_1 q$ fit) versus T and qT, respectively. A subtle temperature dependence is evident in Fig. 3*a*. In particular, the four deviations at 10°C are smaller than the four deviations at 50°C. No similar effect is noted for qT (Fig. 3*b*).

There are apparently two contradictory conclusions for the temperature effect on calibration. The effect is insignificant by the confidence interval test, yet significant for the simple model residual analysis. Our final conclusion was determined by comparing the residual standard deviations (s_{RES}) for the two models shown in Table 6. The residual standard deviation is a measure of quality of fit.

From Table 6, we see that the absolute difference of including the temperature effect improved the fitted model by only a small amount, 0.4 μV. Therefore, the term T (and qT) was omitted in subsequent analyses. It should be noted that the conclusion regarding the statistical insignificance of T applies only to the relatively narrow temperature range under study and such conclusions may not necessarily apply to larger temperature ranges or other types of sensors.

Form of Calibration Equation—A major objective of this study was to assess the linearity of the sensor output (E) with respect to q. Additional calibration measurements were conducted for the large (B) sensors. Based on the analysis of the temperature effect, the large sensors were tested at 20°C and four different levels of heat flux. Table 7 summarizes the results for the six tests.

The data from Tables 3, 4, and 7 are combined and values of E plotted as a function of q (Fig. 4*a*). The plot indicates that E was, in fact, a linear function of q for both small (A) and large (B) sensors. The data for A and B sensors were fit to an equation of the form $E = E_o + Hq$ shown as solid lines in Fig. 3*a*. The intercept term was included to check the significance of our previous results.

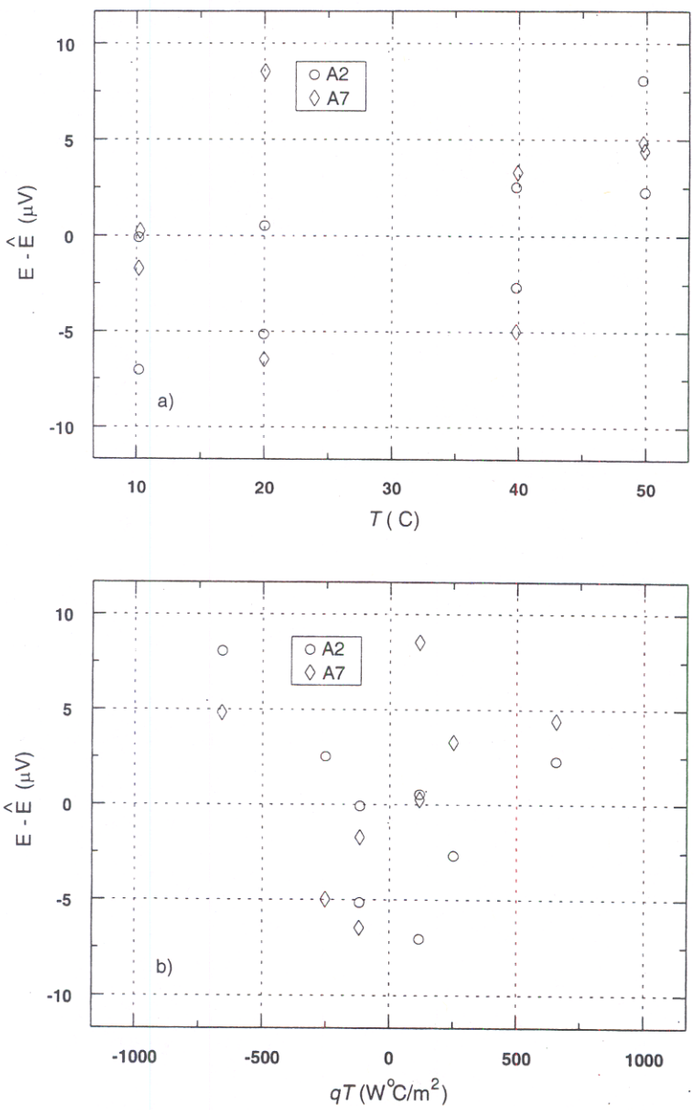

FIG. 3—*Deviations versus independent parameters,* T *and* qT, *for model* E = Hq.

TABLE 6—*Comparison of models.*

Model	s_{RES}, μV
$E = a_1 q$	5.0
$E = a_0 + a_1 q + a_2 T + a_3 qT$	4.6

TABLE 7—*Additional data for large sensors.*

Index	Heat Flux Sensor	T, °C	ΔT, K	q, W/m²	T_1, °C	E, V
1	B12	20.00	10.00	5.867	19.99	0.000810
2	B11	20.00	−20.00	−11.837	20.01	−0.001616
3	B10	20.00	10.00	5.855	n.r.*	0.000802
4	B11	20.00	−10.00	−5.872	19.94	−0.000801
5	B11	20.00	10.01	5.871	19.97	0.000799
6	B11	20.00	20.00	11.829	20.09	0.001617

* Not recorded.

Figure 4*b* shows the deviations (%) from the curve fit ($\hat{E}$) versus q. The deviations for all twelve sensors are less than ±3%, and randomly scattered about zero indicating a satisfactory fit. The necessity for an intercept term can be investigated further by using a curve fit of the form $E = Hq$. Results for the small and large sensors are summarized for the two functional forms in Tables 8*a* and 8*b*.

The estimates for H, corresponding standard deviations ($Std(H)$), and residual standard deviations for the fit (s_{RES}) given in Tables 8*a* and 8*b* confirm that the intercept term is not required and the functional form of $E = Hq$ is sufficient.

Global versus Individual Calibration (Revisited)—Another major objective of this analysis was to confirm our previous results for sensor equivalency by examining the curve fits for different groups of sensors. Tables 9*a* and 9*b* summarize the curve fit statistics for small and large sensors (A and B), respectively.

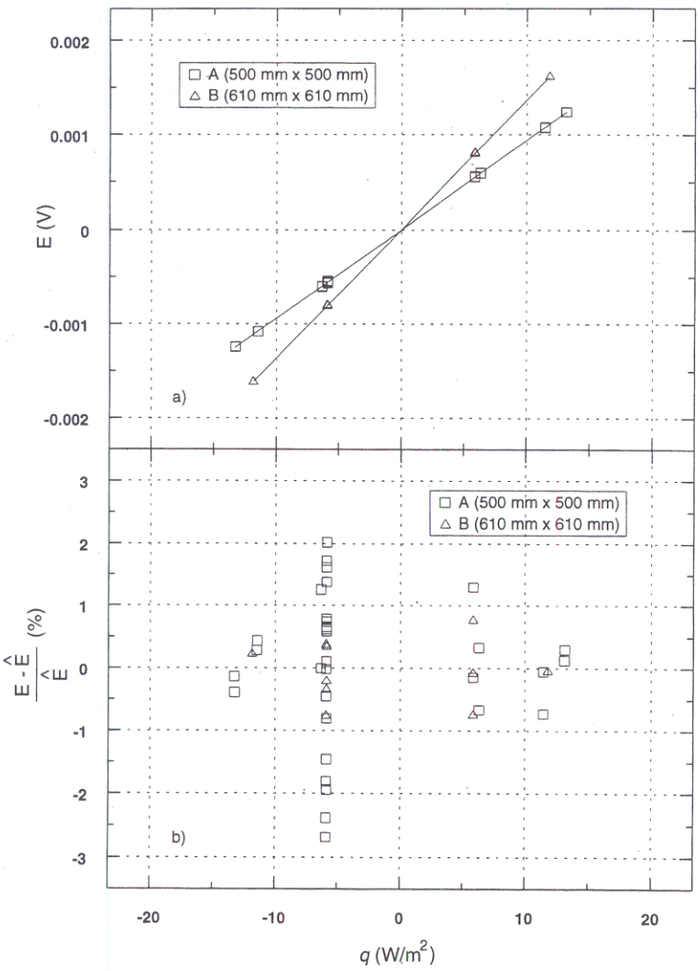

FIG. 4—(a)*Linearity of heat flux sensors (data from Tables 3, 4, and 7),* (b) *Deviations from curve fit versus heat flux.*

TABLE 8a—*Statistical fit parameters for functional form:* E = E_0 + Hq.

Parameter (Units)	Small Sensors A1-A9	Large Sensors B10-B12
n	32	10
E_0 (μV)	1.9	3.4
Std(E_0) (μV)	1.29	1.40
H (μV/(W/m²))	94.1	136.5
Std(*H*) (μV/(W/m²))	0.16	0.19
s_{RES} (μV)	6.8	4.4

TABLE 8b—*Statistical fit parameters for functional form:* E = Hq.

Parameter (Units)	Small Sensors A1-A9	Large Sensors B10-B12
n	32	10
H (μV/(W/m²))	94.0	136.4
Std(H) (μV/(W/m²))	0.15	0.23
s_{RES} (μV)	6.9	5.4

TABLE 9a—*Statistical fit parameters for small sensors (A):* E = Hq.

Parameter	A2	A7	A2&A7	A1-A9
n	10	9	19	32
H (μV/(W/m²))	94.1	94.4	94.3	94.0
Std(*H*) (μV/(W/m²))	0.17	0.18	0.13	0.15
s_{RES} (μV)	5.0	5.0	5.2	6.9

TABLE 9b—*Statistical fit parameters for large sensors (B):* E = Hq.

Parameter (Units)	B11	B10&B11	B10-B12
n	6	8	10
H (μV/(W/m²))	136.3	136.3	136.4
Std(*H*) (μV/(W/m²))	0.25	0.22	0.23
s_{RES} (μV)	5.1	4.7	5.4

The estimates for *H*, corresponding standard deviations (*Std*(*H*)), and residual standard deviations for the fit (s_{RES}) given in Tables 9*a* and 9*b* are quite similar. From an engineering perspective, the results confirm that, across groupings by size, the small and large sensors (A,B) were equivalent.

Final Calibration Equations—In summary, the final calibration equations for the small (A) and large (B) sensors were (1) $\hat{E} = 94.0q$, and (2) $\hat{E} = 136.4q$, respectively.

Uncertainty Analysis

The uncertainty for the calibration results was evaluated using current international guidelines [*8,9*] for the expression of measurement uncertainty. The measurement uncertainty for the estimate of H can be determined by consideration of three primary components: the standard uncertainties for the regression analysis, replication, and the individual measurement contributions. The components are combined by the method of propagation of errors, or

$$u_c = \sqrt{u_1^2 + u_2^2 + u_3^2} \tag{5}$$

Here, u_1 is the standard uncertainty of regression coefficient ($Std(H)$) given in Table 8*b*, u_2 is the standard uncertainty for replicate measurements, and u_3 is the standard uncertainty for the measurement estimate of H (see Appendix).

The standard uncertainty for the regression coefficient is taken as the larger of the values given in Table 8*b*, 0.23 μV/(W/m^2). The standard uncertainty for the replicate measurements is 0.53 μV/(W/m^2) as given earlier. The standard uncertainty for the measurement estimate of H includes uncertainty contributions from E and q and is determined to be 1.4 μV/(W/m^2) as shown in the Appendix. The combined standard uncertainty (Eq 5) is thus 1.5 μV/(W/m^2) or, in relative terms, 1.6 and 1.1% for the small and large sensors, respectively.

Comparison of Test Methods

The primary objective of the comparison was to assess and quantify the equivalency of the test methods. A secondary objective was to quantify the effect of sensor size on H. Four sensors, two from each group in Table 1, were selected randomly and tested daily in a random sequence using C 518 at 24°C and 13 W/m^2. Only one sensor from each group was tested using C 177. The sensors were tested in each apparatus with the same direction of the heat flux through the sensor.

Table 10 summarizes the results. The differences between the average values of H obtained from C 177 and C 518 were −1.1% for A4 and −2.0% for B12. The maximum within-method ranges for H were 0.7% and 1.8% for C 177 and C 518, respectively. By comparison, the "best" expected imprecision indices for C 177 and C 518 are 2 and 3% (2 standard deviation level), respectively. Therefore, the differences between test methods could be considered statistically "equivalent" for many applications. The calibrations presented herein, however, were conducted using C 177 because of the size limitations of C 518 and the requirement for additional calibrations of the apparatus as a function of temperature. As noted in Table 10, values of H for the large sensors (B) are about 49% greater than the small sensors (A).

TABLE 10—*Calibration test method comparison (24°C, ΔT = 22 K).*

	C 177			C 518			
Sensor	n	H (μV/(W/m^2))	Range (%)	n	H (μV/(W/m^2))	Range (%)	Difference (%)
A4	2	91.4	0.7	2	92.4	1.5	−1.1
A9	...	...	...	2	94.3	0.3	...
B10	...	...	...	3	138.3	1.8	...
B12	2	136.8	0.4	3	139.5	0.8	−2.0

Conclusions

This paper addresses four primary issues of interest to the user of C 1130 for the calibration of heat flux sensors for building applications. The calibration measurements were conducted using Test Method C 177 from 10 to 50°C and for a heat flux range of ±13 W/m^2. The twelve sensors were found to be sufficiently equivalent among size categories to allow calibration using a subset of sensors, thus avoiding an extensive calibration requiring many individual measurements. The calibration curve is a linear function that directly relates the sensor output to the applied heat flux. The function does not require an intercept term. The final calibration equations for the small and large sensors are $\hat{E} = 94.0q$ and $\hat{E} = 136.4q$, respectively. The relative combined standard uncertainties are estimated to be 1.6 and 1.1% for the small and large sensors, respectively.

Additional information was determined for the development of precision and bias statements for Practice C 1130. Using Test Method C 177, the repeatability standard deviations determined by pooling data for replicate measurements among small and large sensors were 0.53 μV/(W/m^2) (0.6%) and 0.40 μV/(W/m^2) (0.3%), respectively, at 20°C and 5.9 W/m^2. A comparison of Test Methods C 177 and C 518 indicated agreement within 2%, or better, at 24°C and 5.9 W/m^2. Furthermore, the calibration results obtained using C 177 for the small sensors were within 2% of previous results [*3*]. In view of these results, this particular type of heat flux sensor may serve as a candidate for future interlaboratory testing to determine reproducibility precision indices for Practice C 1130.

Acknowledgments

The authors appreciate the assistance of Susan M. Fioravante with the measurements.

APPENDIX

The combined standard uncertainty for the measurement estimate of H was determined by application of the law of propagation of uncertainty to Eq 1:

$$u_3 = u_c(H) = \sqrt{c_E^2\, u^2(E) + c_q^2\, u^2(q)} \tag{A-1}$$

The sensitivity coefficients, c_i, are the partial derivatives of Eq 1 with respect to E and q evaluated at their respective input estimates. Recall that for C 177, q was determined directly from the electrical power input (Q) to the apparatus metre area divided by metre area (A), or $q = Q/A$. The combined standard uncertainty for the measurement estimate of q was determined from

$$u_c(q) = \sqrt{c_Q^2\, u^2(Q) + c_A^2\, u^2(A)} \tag{A-2}$$

The uncertainty budget for the determination of q is given in Table A1. The estimates for Q and A were 0.7636 W and 0.129748 m^2. The standard uncertainty for $u(Q_g)$ was taken from a previous series of experiments [*10*].

The uncertainty budget for the determination of H is given in Table A2. The estimates used for E and q were 0.000551 V and 5.866 W/m^2. The combined standard uncertainty for the measurement estimate of H was 0.0000014 V/(W/m^2), or 1.4 μV/(W/m^2).

TABLE A1—*Summary of standard uncertainty components for* q.

Source of Uncertainty	u_i	c_i
(1) repeated observations (pooled), $u(Q_{mean})$	0.00050 W	1
(2) uncertainty of voltage, current measurements, $u(V, i)$	0.00083 W	1
(3) deviation from one-dimensional heat flow, $u(Q_g)$	0.00980 W	1
(4) combined standard uncertainty, $u(Q)$	0.00985 W	$1/A$
(5) metre area, $u(A)$	0.000023 m^2	$-Q/A^2$
Combined standard uncertainty, $u_c(q)$	0.0759 W/m^2	

TABLE A2—*Summary of standard uncertainty components for* H.

Source of Uncertainty	u_i	c_i
(1) repeated observations (pooled), $u(E_{mean})$	0.000002 V	1
(2) digital voltmeter, $u(E_1)$	−0.000002 V	1
(3) offset voltage for connection card, $u(E_2)$	0.000003 V	1
(4) combined standard uncertainty, $u(E)$	0.000004 V	$1/q$
(5) combined uncertainty, $u(q)$	0.0759 W/m^2	$-E/q^2$
Combined standard uncertainty, $u_c(H)$	0.0000014 $V/(W/m^2)$	

References

[1] Fanney, A. H. and Dougherty, B. P., "Building Integrated Photovoltaic Test Facility," *Proceedings of the ASES, NPSC, AIA, ASME, MREA Conference Solar 2000,* 16–21 June 2000.

[2] Manual on the Use of Thermocouples in Temperature Measurement; *ASTM Manual 12,* ASTM, Philadelphia, PA, 1993.

[3] Degenne, M. and Klarsfeld, S., "A New Type of Heat Flowmeter for Application and Study of Insulation and Systems," *Building Applications of Heat Flux Transducers, ASTM STP 885,* E. Bales, M. Bomberg, and G. E. Courville, Eds., American Society for Testing and Materials, Philadelphia, 1985, pp. 163–171.

[4] Zarr R. R., "Control Stability of a Heat-Flow-Meter Apparatus," *Journal of Thermal Insulation and Building Envelopes,* Vol. 18, October 1994, pp. 116–127.

[5] Lackey, J., Normandin, N., Marchand, R., and Kumaran, K., "Calibration of a Heat Flow Meter Apparatus," *Journal of Thermal Insulation and Building Envelopes,* Vol. 18, October 1994, pp. 128–144.

[6] Flanders, S. N., "Heat Flow Sensors on Walls—What Can We Learn?" *Building Applications of Heat Flux Transducers, ASTM STP 885,* E. Bales, M. Bomberg, and G. E. Courville, Eds., American Society for Testing and Materials, Philadelphia, 1985, pp. 140–159.

[7] Powell, F. J. and Rennex, B. G., "Workshop on Laboratory Use of Heat Flux Transducers," *Building Applications of Heat Flux Transducers, ASTM STP 885,* E. Bales, M. Bomberg, and G. E. Courville, Eds., American Society for Testing and Materials, Philadelphia, 1985, pp. 245–249.

[8] ANSI, "U.S. Guide to the Expression of Uncertainty in Measurement," *ANSI/NCSL Z540-2-1997,* 1997.

[9] Taylor, B. N. and Kuyatt, C. E., "Guidelines for Evaluating and Expressing the Uncertainty of NIST Measurement Results," *NIST Technical Note 1297,* 1994.

[10] Zarr, R. R., "Glass Fiberboard, SRM 1450c, for Thermal Resistance from 280 K to 340 K," *NIST Special Publication 260-130,* 1997.